Journal of Materials Chemistry C

Optically stable and tunable quantum dot nanocrystals embedded cholesteric liquid crystal composite laser

Journal:	*Journal of Materials Chemistry C*
Manuscript ID:	TC-ART-01-2014-000128.R1
Article Type:	Paper
Date Submitted by the Author:	09-Mar-2014
Complete List of Authors:	Lin, Lin-Jer; Dept. of Photonics, Dept. of Photonics Lin, Jia-De; Dept. of Photonics, Dept. of Photonics Lee, Chia-Rong; Dept. of Photonics, Dept. of Photonics

Journal of Materials Chemistry C

Cite this: DOI: 10.1039/c0xx00000x

PAPER

www.rsc.org/xxxxxx

Optically stable and tunable quantum dot nanocrystals embedded cholesteric liquid crystal composite laser

Lin-Jer Chen, Jia-De Lin, and Chia-Rong Lee*

Received (in XXX, XXX) Xth XXXXXXXXX 20XX, Accepted Xth XXXXXXXXX 20XX
DOI: 10.1039/b000000x

This investigation first reports an optically stable and tunable laser using quantum-dots (QD) embedded cholesteric liquid crystal (QD-CLC) microresonator added with a chiral-azobenzene. The QD nanocrystal, CLC, and chiral-azobenzene play various key roles in the highly stable fluorescence nano-emitter, microresonator, and photo-tuner in the photonic bandgap (PBG) of the CLC and associated lasing output, respectively. Experimental results show that both the PBG and lasing emission of the QD-CLC composite sample can be reversibly tuned under successive irradiation of UV and blue beams. The all-optical tunability of the laser is attributable to successive elongation and shrinkage back of the CLC pitch induced by UV- and blue-beam-irradiation induced *trans-cis* and *cis-trans* back isomerizations of chiral-azobenzene, respectively. In addition, this composite laser has a high damage threshold (> 85 μJ/pulse), and thus shows a highly optical stable uniquness. This work successfully opened up an opportunity for developing QD coherent light sources or lasers with a compatibility of optical stability and tunability (e.g., optical stable and tunable single photon lasers).

1 Introduction

Quantum-dot nanocrystals (QD NCs) are characterized by a number of unique physical properties that originate from the quantum confinement effect of their reduced dimension.[1] Especially, as an optically emitting media, they holds lots of advantages in fabrication of QD LEDs or lasers, such as high efficiency, sharp emission, long-termed stability, decreased lasing threshold and relative intensity noise, and temperature insensitivity.[2-5] QD lasers are semiconductor lasers in which the QD NCs are regarded as a gain medium. In contrast with the colloidal NCs based QDs used in the present study, the conventional inorganic QD lasers were fabricated by using molecular beam epitaxy (MBE) or metalorganic chemical vapor deposition (MOCVD) to form self-assembled QDs via Stranski-Kastranow growth mode.[6-9] Although traditional QD lasers have many advantages as mentioned above, deficiencies in aspect of flexible tunabilities in lasing features by externalities (e.g., heat, stress, electrical and optical fields) significantly limit the QD lasers in applications if they are fabricated completely.

Cholesteric liquid crystal (CLC) is a special soft-matter with a highly index-modulated spiral structure, in which the rod-like LC molecules can self-organize to rotate periodically with a repetition of pitch along a helical axis. As a result, CLC can be regarded as a one-dimensional (1-D) photonic bandgap (PBG) material.[10] In addition, CLC has been highlighted in virtue of its highly flexible tunability by using various methods, e.g., applying voltage and stress, heating/cooling, illumination of actinic light, and changing pumped position, and potential applications, such as dye-doped CLC (DDCLC) lasers.[11-15]

The azobenzene materials have attracted considerable attention in recent decades in virtue of their intriguing mechanism of photoisomerization, and potential applications in optical switches and memory storage, molecular machines, nanodevices, and biochemical activity. In addition, they have lots of merits, such as clean and rapid photochemical reaction, thermal stability, photo-reversibility, and so on.[16-21] As depicted in Scheme 1, the azobenzene dopant of chromophores is characterized by the azo linkage (–N=N–) that bridges two phenyl rings.[19] Two isomeric states may exist for the azobenzene chromophores, the thermodynamically stable *trans* isomer and the meta-stable *cis* isomer. The structures of the two isomers are different mainly in the direction of their central bonds. In *trans* state, the two bonds linking the azo group to the phenyl rings are parallel, resulting in an rod-like molecule. In *cis* state, the included angle between the two bonds is 120 degrees, leading to a molecule with V-like shape. The absorption spectra of azobenzene molecules generally exhibit their absorption maxima at UV and visible regions (around 350 and >420 nm, respectively) due to the π-π* and n-π* transitions, respectively. The azobenzene can be reversibly transformed by rapid *trans-cis* and *cis-trans* back isomerizations under the irradiation of UV and visible lights, respectively. Alternately, the meta-stable *cis* isomers can also spontaneously

convert to *trans* form via relatively slow thermal relaxation (Δ). The concentration ratio of *cis* and *trans* isomers is dependent on the quantum yields of the *trans-cis* and the reverse *cis-trans* photoisomerization reactions. Two various mechanisms have been proposed for photoisomerization of azobenzene: the *trans-cis* isomerization via rotation about the –N=N– bond and *cis-trans* isomerization via inversion of one of the nitrogen atoms in the same molecular plane.[21] Because of the above-mentioned merits, the azobenzene materials are extensively used in optically controlled LC-based devices via the interaction between the azobenzene and LC molecules in various LC phases such as nematic, cholesteric, and blue phases.[16]

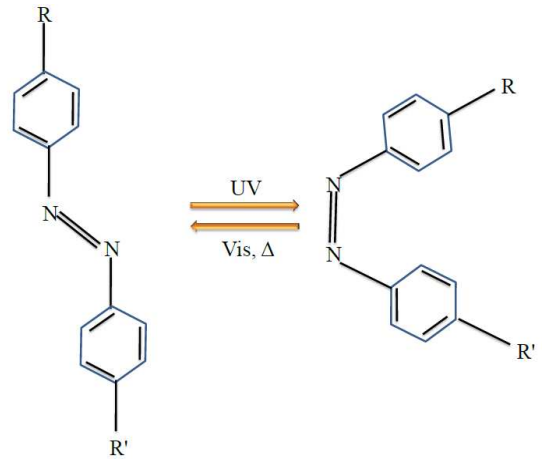

trans isomer *cis* isomer

Scheme 1. Typical configurations of *trans* (left) and *cis* (right) isomers and *trans-cis* isomerization of the azobenzene molecule. R and R' are chemical functional groups.

There are some investigations emerged recently based on complex materials with inorganic QD NCs and organic CLCs, in which their individual merits in high stability and highly flexible tunability, respectively, are cleverly merged. Bobrovsky *et al.* developed a controllable fluorescence emitter which can optically and electrically control the circularly polarized emission from QDs in CLC.[22] Rodarte *et al.* demonstrated spectral and polarization modulation of QD photoluminescence by the selective PBG of CLC matrix.[23] Lukishova *et al.* demonstrated that the fluorescence from QDs in near-IR region can be amplified in CLC microresonator under cw excitation.[24] Moreover, Lee and coworkers have successfully demonstrated a thermally and electrically tunable lasing emission and amplified spontaneous emission in visible region based on a QD embedded CLC (QD-CLC) composite cell very recently.[25] In the QD-CLC composite laser, the QD functions not only as a gain medium but also as an effective stabilizer of CLC structure because of the intrinsically high stability of the QDs and their interactions with the LC molecules. The stability of the QD-CLC composite laser demonstrates the toleration of a strong pumped energy without damage (over 83 μJ/pulse), and this threshold is over 1.66 times higher than the damage threshold (50 μJ/pulse) of a traditional DDCLC laser. In spite of the fact that the lasing features (e.g., lasing threshold) of the QD-CLC laser are poor than those of DDCLC laser at the present stage, it is worth to go deep into further study of the QD-CLC laser and its tuning applications because of its high stability and reliability which are deficiently in DDCLC systems due to the inherently significant drawbacks of the system, e.g., the strong photobleaching of the organic dye and concomitantly strong thermal effect induced instability and thermal damage of the system during excitation.

As mentioned previously, the CLC is known to be a PBG material with a highly flexible tunability. Among those methods for tuning, photo-control has advantages over others, such as easy addressability, fast response time, remote control in various ambient environments, precise and reversible control with using neat and green light, and a great diversity of adjustable factor of the actinic light, e. g., intensity, polarization, wavelength, phase retardation, interference, and so on.[26] To achieve the purpose of photo-tuning CLC, an effective way is to add a small amount of photoresponsive material into the CLC host.[27-29] Azobenzene matters in which photoisomerizable phenomenon are dominative are mostly representative in such photoresponsive materials.[30, 31] Among azo-materials, chiral-azobenzene is especially unique because of its advantages such as ease of reversible photo-tuning of CLC and wide tuning range in spectrum.[32]

In addition, the stability in PBG and lasing output for traditional DDCLC systems were usually achieved by using the polymer network stabilized method. However, the increase of stability by polymer network may lead to the almost complete loss of external tunability once the cell fabrication has been completed in virtue of the strongly fixed effect of the polymer chains in local LC orientations and thus in the pitch of the CLC.[33, 34] The merits of stability and tunability seem to be incompatible in traditional DDCLC systems either with or without polymer network. In this article, we report for the first time an optically stable and tunable QD-CLC composite laser device added with a chiral-azobenzene. The QD, CLC, and chiral-azobenzene play various key roles in fluorescence nano-emitter with a high stability, microresonator, and photo-tuner in the PBG of the CLC and thus in the lasing signal, respectively. The QD-CLC devices have a potential to be developed as coherent light sources or laser devices with compatible optical stability and tunability (e.g., optically stable and tunable single photon lasers).

2 Experimental

The CLC mixtures used in this study include nematics (MDA-03-3970), chiral-azobenzene (4-Ethoxy-4'-citronellyloxyazobenzene, ChAD-2-S, left-handedness; from BEAM) and chiral host (S811, left-handedness; from Merck). Figure 1 shows the molecular structures of the chiral-azobenzene with *trans* and *cis* forms. The *trans* isomer can convert to the *cis* state via UV-irradiation induced *trans-cis* isomerization. The *cis* isomer can transform back to the *trans* state via blue-light-irradiation induced *cis-trans* isomerization or thermal *cis-trans* back isomerization. The weight ratio of nematics, chiral-azobenzene and chiral host is 70.52:4.13:16.63 *wt*% in the prepared CLC mixtures. The 8.7 *wt*% CdSe/ZnS NC QDs with a CdSe core and a ZnS shell (average diameter ≅ 3 nm, from PlasmaChem, Quantum Yield ≅

Department of Photonics and Advanced Optoelectronic Technology Center, National Cheng Kung University, Tainan, Taiwan 701, E-mail: crlee@mail.ncku.edu.tw

85%) are then added in the CLC mixture and attempted to homogenize by ultrasonic oscillation for 2 days. The surface of each QD is pre-decorated with the surfactant TOPO (Trioctylphosphine oxide, $OP(C_8H_{17})_3$) for preventing from a serious aggregation among the QD NCs. An empty cell is pre-built by piling up two glass substrates, separated by spacers with a thickness of 50 μm. The inner surfaces of the cell substrates were pre-coated with polyvinylalcohol films and rubbed along the same direction. The QD-CLC mixture was injected into the empty cell at an isotropic temperature of 95 °C and then slowly cooled down to room temperature. As displayed in Fig. 2(a), a planar CLC texture with some oily streaks can be observed in the cell under the polarizing optical microscope (POM) with crossed polarizers. Figure 2(b) shows the fluorescence microscope image of the QD-CLC. Clearly, only a few microscopic aggregates of QD present in the cell. That is, the aggregation effect among QD NCs in the cell doped with the high QD concentration (8.7 *wt*%) is weak. Therefore, a quite homogeneous dispersion for a majority of NCs can be obtained. This is probably attributed to the surfactant-induced passivation of QDs in the cell, which effect may indirectly enable the first success of the lasing emission in the present QD-CLC.

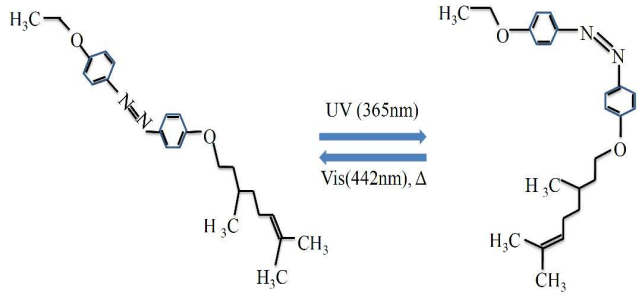

trans isomer *cis* isomer

Fig. 1 Molecular structures of the chiral-azobenzene (ChAD-2-S) with *trans* (left) and *cis* (right) forms.

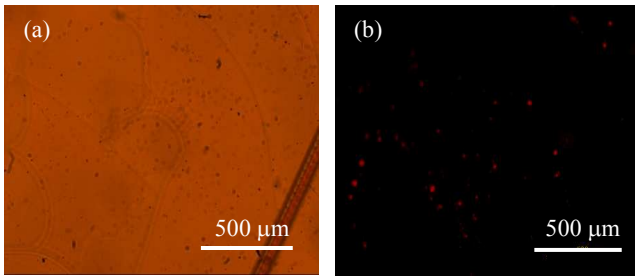

Fig. 2 Microscopic images of QD-CLC cell measured under (a) POM with crossed polarizers and (b) fluoresence microscope.

The fluorescence or lasing emission of the QD-CLC is measured after the excitation of the pumped pulses in the experimental setup shown in Fig. 3. A second harmonic-generated pumped pulses from a Q-switch Nd:YAG laser, with a wavelength, pulse width, and pulse repetition frequency of 532 nm, 8 ns, and 10 Hz, respectively, is used to normally pump the QD-CLC cell. The incident beam was focused on the sample by a lens (focal length: 20 cm) along +z direction. The induced lasing emission along the +z direction of the cell was measured behind the cell by using a fiber-based spectrometer with an optical resolution of ~1.0 nm (Jaz-combo-2, Ocean Optics). A notch filter (for 532 nm) is placed behind the cell to block the strong transmitted light of the pumped pulses from directly damaging the spectrometer. A half-wave plate (λ/2 wave-plate for 532 nm) and a polarizer are placed behind the exit of the laser to adjust the incident pumped energy (E) of the pumped pulses on the cell. The reflection spectrum of the incident white light that is illuminated at normal incidence on the QDCLC is also obtained using a same spectrometer system to identify the PBG of the QD-CLC. One UV beam and one blue laser beam (He-Cd laser, 442 nm) successively irradiate the cell at angles of 30° and 40° relative to +z direction, respectively, for performing the experiment of all-optically tuning the PBG and lasing signal of the QD-CLC.

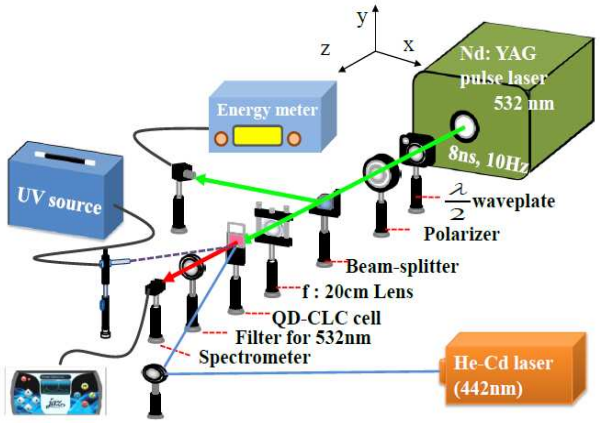

Fig. 3 Experimental setup for measuring the fluorescence or lasing emission of chiral-azobenzene added QD-CLC laser and its all-optical controllability by successive irradiations of UV beam and blue laser beam from a He-Cd laser (λ = 442 nm).

3 Results and discussions

Figure 4(a) shows the pre-measured absorption and fluorescence emission spectra of 8.7 wt% QD dissolved in a toluene solution with a molar concentration of ~5×10^{-5} mol/cm^3 (black and blue curves, respectively) and the pre-measured emission spectrum of QD-CLC in isotropic phase (red curve). The absorption spectra are obtained using a UV-visible spectrometer (U-4100, from HITACHI). The peak wavelengths of the fluorescence emission appeared in the two samples are the same at around 613 nm. The long-wavelength-edge (LWE) of the CLC PBG is adjustable to be located within the fluorescence band of the QD such that efficient amplification of the fluorescence can be obtained.

Figure 4(b) shows the variations of the fluorescence emission intensity and corresponding full width at half maximum (FWHM) for the lasing peak at around 598 nm based on QD-CLC added with the chiral-azobenzene. Apparently, the fluorescence emission increases abruptly and the FWHM abruptly decreases to a steady value of ~1.1 nm when the pumped energy exceeds a threshold value of E_{th} = 35 μJ/pulse. This is a symptom for the occurrence of a lasing emission. The occurrence of the lasing emission mainly counts on the stable gain medium of QD nano-emitters. The QDs can spontaneously emit fluorescence photons

via the stimulus of the pumped pulses. The fluorescence photons with wavelengths nearly at the LWE of the PBG of the CLC microcavity have a very high density of photonic state and a very low group velocity such that the dwelling time of the photons in the CLC is very long. This can dramatically enhance both the rates of spontaneous and stimulated emissions, resulting in a high gain which exceeds the loss, and therefore the generation of a lasing emission. To test the optical stability of the QD-CLC composite laser, the above-mentioned measurement is performed with three rounds (shown in Fig. 4(b) by triangle, circle, and square points for first, second and third rounds, respectively). The cell clearly shows little change in its lasing characteristics in the three rounds even if the pumped energy can be as high as 85 μJ/pulse, which energy is usually significantly higher than the damage threshold of a traditional DDCLC laser.[25] This result demonstrates a highly optical stability in the present QD-CLC composite laser.

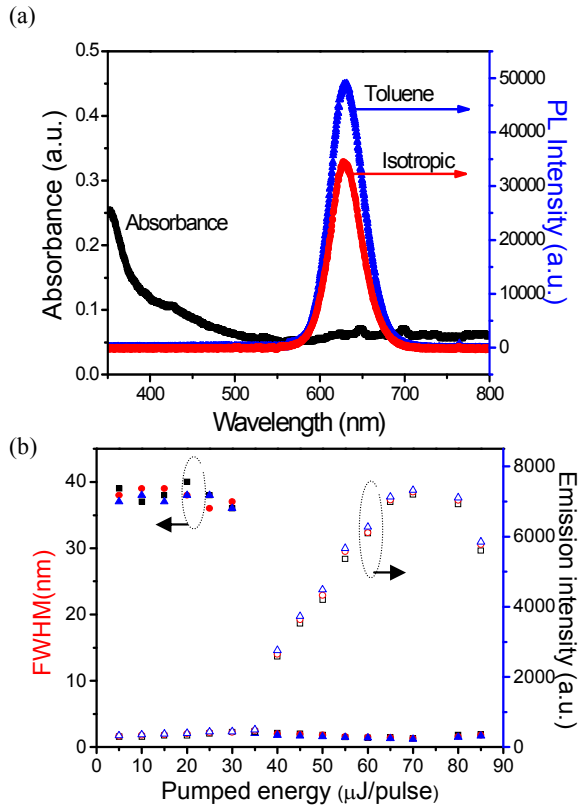

Fig. 4 (a) Measured fluorescence emission and absorption spectra of 8.7 *wt*% QD dissolved in toluene (blue and black curves, respectively) and the measured fluorescence emission of the QD-CLC cell in isotropic phase (red curve). The emission spectrum of the QD is obtained under the excitation of a diode-pumped solid-state laser with wavelength of 532 nm and intensity of 150 μW/cm^2. (b) Variations of the emission intensity and corresponding FWHM for the emission peak at ~598 nm with pumped energy in the QD-CLC added with a chiral-azobenzene. To test the optical stability of the QD-CLC laser, the above-mentioned measurement is repeated for three rounds. The data associated with the fluoresnece emission intensity (FWHM) for first, second and third rounds are labeled by hollow (solid) triangle, circle, and square points, respectively.

Figure 5(a) presents the evolution for optically tuning the lasing wavelength of the QD-CLC composite laser added with the chiral-azobenzene at E = 50 μJ/pulse which exceeds E_{th} under the UV irradiation with a fixed intensity of 1.5 mW/cm^2. The lasing peak continuously red-shifts from 598 nm to 638 nm with increasing the irradiation time from t_{UV} = 0 to t_{UV} = 7 min. The tuning band is just included within the fluorescence band of the QD nano-emitters. Whereas experimental result in an additional experiment (not shown herein) shows that no tuning feature can be observed based on a QD-CLC cell with no chiral-azobenzene, one can ensure that the chiral-azobenzene plays a key role in the optical tuning of the lasing emission (Fig. 5(a)) based on the QD-CLC cell added with the chiral-azobenzene.

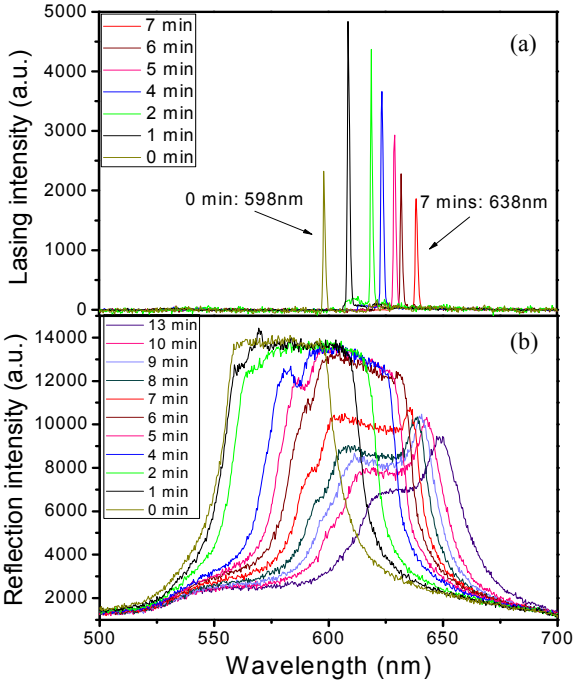

Fig. 5 (a) Optical tuning of the lasing emission of the QD-CLC laser added with the chiral-azobenzene under the UV irradiation with 1.5 mW/cm^2 for 7 mins. The pumped energy used is E = 50 μJ/pulse, which exceeds E_{th}. (b) Optically induced red-shift of the reflection band of the chiral-azobenzene added QD-CLC under the UV irradiation of 1.5 mW/cm^2 for 13 mins.

To understand the underlying mechanism of the optical tunability of the QD-CLC composite laser, the reflection spectra of the QD-CLC cell added with the chiral-azobenzene is measured after the cell is illuminated by the UV beam with 1.5 mW/cm^2 at t_{UV} = 0 ~ 13 min. Figure 5(b) shows associated experimental result. A continuous red-shift of the reflection band of the QD-CLC cell is obtained, where the LWE of the PBG may be optically tuned continuously from roughly 598 nm to 653 nm, at increasing t_{UV} from 0 to 13 min. The red-shift of the LWE of the CLC PBG under the UV irradiation is the reason for the optical tuning evolution of the lasing peak of the QD-CLC cell. The red-shift of the CLC PBG is attributable to the UV-irradiation induced *trans-cis* isomerization of the chiral-azobenzene molecules. Generally, the azo-chiral molecule probably exists at a stable *trans* state and a metastable *cis* state.

The absorption spectra of the azo-chiral molecules for the two states are quiet different. As described in the previous literature,[35] the chiral-azobenzene has two absorption bands with peak wavelengths at 365 and 442 nm, associated with π-π* and n-π* transitions, respectively. Figure 6 further shows the schematic illustration for explaining the mechanism of the optical tunability of the QD-CLC composite cell via the photoisomerization of the chiral-azobenzene. In dark, all the azo-chiral molecules tend to be at stable *trans* state. After the UV irradiation on the cell, the concentration of the *trans* isomer decreases and that of the *cis* isomer increases simultaneously, resulting in the absorption peaks at 365 and 422 nm drops and rises, respectively. Because the handednesses for chiral host S811 and chiral-azobenzene are the same in the same NLC, the resultant HTP value of the entire cell is the sum of their individual HTP values. Once the UV beam irradiates the cell, the rod-like *trans* azo-chiral molecules which originally align along the LC molecular axes may transform to curve *cis* isomers via *trans-cis* photoisomerization effect. The *cis* isomers with a curve configuration and random orientations for the chiral-azobenzene can locally disturb the CLC molecules and decreases the local order parameter of the LCs (See the insets in Fig. 6), resulting in the decrease of the HTP value of the chiral-azobenzene. This can cause the decrease of the resultant HTP value of the QD-CLC cell and thus the elongation of the pitch, leading to the red-shift of the PBG and thus of the lasing peak of the QD-CLC composite laser under the UV irradiation. This red-shift can stop when the dynamic balance between the concentrations of *trans* and *cis* isomers reaches during the UV irradiation. Notably, no lasing can be acquired when the LWE of the PBG exceeds 638 nm. This is because of the significant deformation of the PBG (Fig. 5(b)) and thus of the PC-like structure of the planar CLC after the UV-irradiation-induced serious disturbance of the curve *cis* isomers of the chiral-azobenzene with a high concentration over 7 mins.

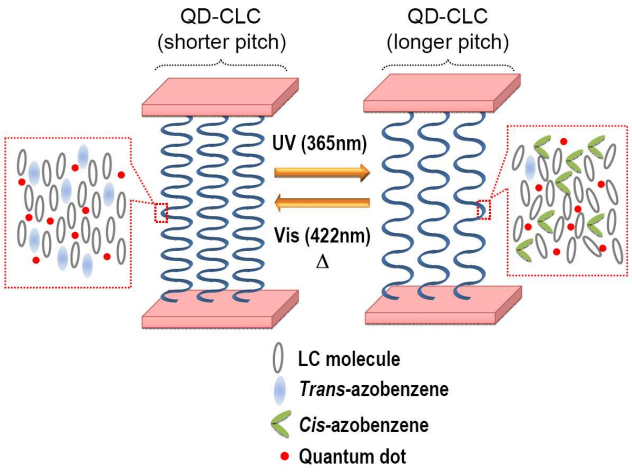

Fig. 6 Schematic illustration for explaining the mechanism of the optical tunability of the QD-CLC composite cell via the photoisomerization of the chiral-azobenzene. The chiral host molecules (S811) are not depicted in the QD-CLC.

To prove the significant deformation of the planar CLC and thus of the PBG, this work also detects the microscopic morphology of the QD-CLC cell under the same condition of UV irradiation. Figure 7 shows the microscopic morphological images of the QD-CLC cell under POM with crossed polarizers at t_{UV} = 0, 3, 6, 7, 8, and 10 min. Clearly, the CLC presents a planar texture at $t_{UV} \leq 6$ min, resulting in the less deformation of the PBG structure. However, at $t_{UV} \geq 7$ min, an apparent deformation of CLC texture with many uniformly distributed microdroplets forms, resulting in the significant deformation of PBG. The formation of these microdroplets is primarily attributable to the local significant perturbation of the long-termed (≥ 7 mins) UV-irradiation-induced accumulative *cis* chiral-azobenzene molecules on the CLC helical texture.[35] It is, therefore, interpretable that no lasing emission appears at $t_{UV} > 7$ min.

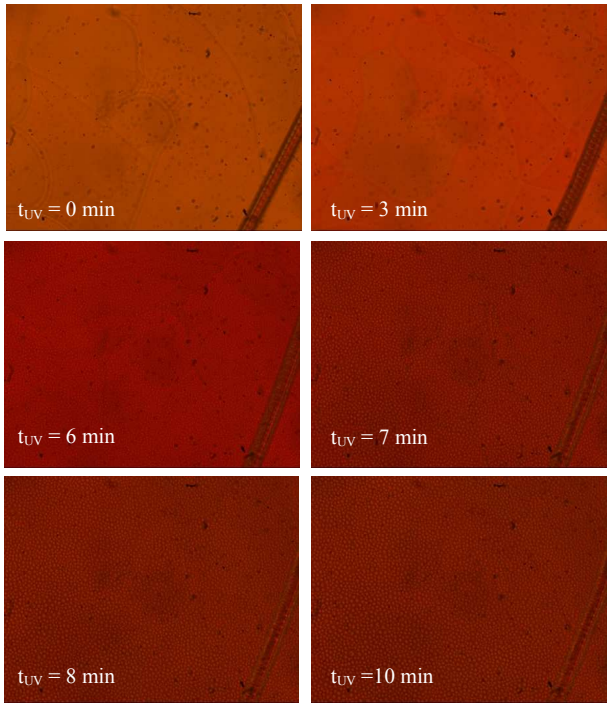

Fig. 7 Measured morphological images of QD-CLC cell under POM with crossed polarizers under the sussesive irradiation of the UV beam irradiation with 1.5 mW/cm^2 from t_{UV} = 0 to t_{UV} = 10 min.

In addition to the tunable feature of the QD-CLC composite laser under UV irradiation, this work also measures the lasing spectra individually under the irradiation of the blue laser beam with 1.6 mW/cm^2 and in natural relaxation following the UV irradiation for 7 mins. Associated results are summarized into the variations of the lasing wavelength with the irradiation times of the UV and blue beams (t_{UV} and t_B, respectively) and the natural relaxation time in dark (t_{relax}), and shown in Fig. 8. Apparently, the UV irradiation may induce the lasing peak to red-shift from 598 nm to 638 nm in 7 mins (indicated by dots "▲"), and the blue-beam irradiation and natural relaxation may lead to the lasing peak to blue-shift back in 10 and > 30 mins, respectively (indicated by dots "■" and "●", respectively). Actually, the complete recovery of the lasing peak to the original wavelength (598 nm) in dark spent one day which is much longer than that by the recovery of the blue-beam irradiation. This is because the rate of photoinduced *cis-trans* back isomerization for azo-materials is

significantly faster than the rate of thermal *cis-trans* back isomerization. The curve *cis* isomers of the chiral-azobenzene may quickly (slowly) transform back the rod-like *trans* form under the blue-beam irradiation (in dark), and quickly (slowly) restabilize the LCs, resulting in the fast (slow) recovery of the resultant HTP value of S811 and ChAD-2-S in NLC and thus the fast (slow) shrinkage back of the pitch. In turn, the PBG and thus the lasing peak quickly (slowly) recovers back to the original state.

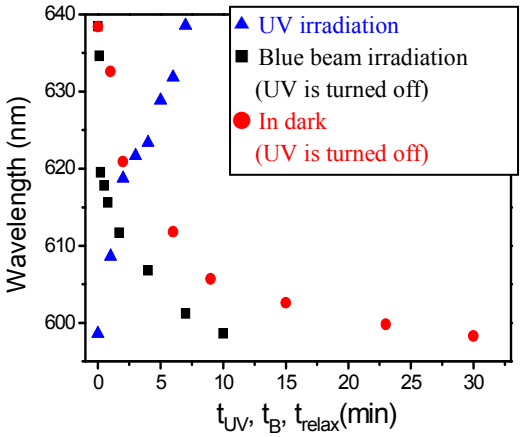

Fig. 8 Variations of the lasing wavelength of the QD-CLC laser with irradiation time (t_{UV}) of UV beam with 1.5 mW/cm^2 (indicated by dots "▲") and with irradiation time (t_B) of blue beam with 1.6 mW/cm^2 and natural relaxation time (t_{relax}) in dark (indicated by dots "■" and "●", respectively) following the UV irradiation. The moment is set as $t_B = t_{relax} = 0$ once the UV irradiation is turned off.

4 Conclusions

In conclusion, this work demonstrates for the first time a QD-CLC composite laser added with a chiral-azobenzene with a compatibility of optical stability and tunability. The lasing wavelength of the QD-CLC composite laser can be reversibly tuned by successive irradiation of one UV beam and one blue laser beam due to original mechanisms of UV-irradiation-induced *trans-cis* isomerization and blue-beam-induced *cis-trans* back isomerization, respectively. The tunable spectral range in PBG and lasing wavelength of the QD-CLC composite cell is over 60 and 40 nm, respectively. Because of the high stability and optical and electrical dual-excitability of QDs, the QD-CLC has a high potential to develop a multi-way-drivable coherent QD light sources or lasers with a highly flexible tunability and a high stability and reliability (e.g., single photon lasers with high tunability, stability, and reliability).

Acknowledgements

The authors would like to thank the National Science Council of the Republic of China, Taiwan (NSCT) (contract NSC 100-2112-M-006-012-MY3) and the Advanced Optoelectronic Technology Center, National Cheng Kung University, under projects from the Ministry of Education, for financially supporting this research.

Notes and references

1 A. P. Alivisatos, *Science*, 1996, **271**, 933.
2 H. V. Demir, S. Nizamoglub, T. Erdemb, E. Mutluguna, N. Gaponikc, and A. Eychmullerc, *Nano Today*, 2011, **6**, 632.
3 Y. Zhao, C. Riemersma, F. Pietra, R. Koole, C. de Mello Donega, and A. Meijerink, *ACS Nano*, 2012, **6**, 9058.
4 L. Sun, J. J. Choi, D. Stachnik, A. C. Bartnik, B. R. Hyun, G. G. Malliaras, T. Hanrath, and F. W. Wise, *Nature Nanotechnology*, 2012, **7**, 369.
5 T. Erdem and H. V. Demir , Nat. *Photonics*, 2011, **5**, 126.
6 G. Ozgur , A. Demir and D. G. Deppe , *IEEE J. Quantum Electron*., 2009, **45**, 1265.
7 Y. K. Ee , H. Zhao , R. A. Arif , M. Jamil and N. Tansu , *J. Crystal Growth*, 2008, **310**, 2320.
8 G. Liu , H. Zhao, J. Zhang , J. H. Park , L. J Mawst, and N. Tansu , *Nanoscale Res. Lett.*, 2011, **6**, 342.
9 V. I. Klimov, A. A. Mikhailovsky, S. Xu, J. A. Hollingsworth, C. A. Leatherdale, H. J. Eisler and M. G. Bawendi, *Science*, 2000, **290**, 314.
10 S. Furumi, S. Yokoyama, A. Otomo, and S. Mashiko, *Appl. Phys. Lett.*, 2004, **84**, 2491.
11 Y. Huang, Y. Zhou, C. Doyle, and S.-T. Wu, *Opt. Express*, 2006, **14**, 1236.
12 Y. Matsuhisa, Y. Huang, Y. Zhou, S.-T. Wu, R. Ozaki, Y. Takao, A. Fujii, and M. Ozaki, *Appl. Phys. Lett.*, 2007, **90**, 091114.
13 K. Dolgaleva, S. K. H. Wei, S. G. Lukishova, S. H. Chen, K. Schwertz, and R. W. Boyd, *J. Opt. Soc. Am. B*, 2008, **25**, 1496.
14 C. R. Lee, S. H. Lin, H. C. Yeh, T. D. Ji, K. L. Lin, T. S. Mo, C. T. Kuo, K. Y. Lo, S. H. Chang, and Y. G. Fuh, and S. Y. Huang, *Opt. Express*, 2009, **17**, 12910.
15 H. Coles, and S. Morris, *Nature Photonics*, 2010, **4**, 676.
16 F. Simoni, and O. Francescangeli, *J. Phys.: Condens. Matter*., 1999, **11,** R439.
17 T. Fujino, and T. Tahara, *J. Phys. Chem. A*, 2000, **104**, 4203.
18 G. S. Kumar, and D. C. Neckers, *Chem. Rev.*, 1989, **89**, 1915.
19 Y. Yu, and T. Ikeda, *J. Photochem. Photobiol. C: Photochem. Rev.*, 2004, **5**, 247.
20 T. J. White, M. E. McConney, and T. J. Bunning, *J. Mater. Chem*., 2010, **20**, 9832.
21 C. W. Chang, Y. C. Lu, T. T. Wang, and E. W. G. Diau, *J. Am. Chem. Soc.*, 2004, **126**, 10109.
22 A. Bobrovsky, K. Mochalov, V. Oleinikov, A. Sukhanova, A. Prudnikau, M. Artemyev, V. Shibaev, and I. Nabiev, *Adv. Mater*., 2012, **24**, 6216.
23 A. L. Rodarte, C. Gray, L. S. Hirst, and S. Ghosh, *Phys. Rev. B*, 2012, **85**, 035430.
24 S. G. Lukishova, L. J. Bissell, J. Winkler, and C. R. Stroud Jr., *Opt. Lett.*, 2012, **37**, 1259.
25 L. J. Chen, J. D. Lin, S. Y. Huang, T. S. Mo, and C. R. Lee, *Adv. Opt. Mater.*, 2013, **1**, 637.
26 Q. Li, Liquid Crystals Beyond Displays; Chemistry, Physics, and Applications, John Wiley & Sons, Inc., Hoboken, New Jersey, 2011.
27 H. K. Lee, A. Kanazawa, T. Shiono, T. Ikeda, T. Fujisawa, M. Aizawa, and B. Lee, *Chem. Mater.*, 1998, **10**, 1402.

28 C. R. Lee, J. D. Lin, Y. J. Huang, S. C. Huang, S. H. Lin, and C. P. Yu, *Opt. Express*, 2011, **19**, 9676.
29 B. N. Feringa, N. P. M. Huck, and A. M. Schoevaars, *Adv. Mater.*, 1996, **8**, 681.
30 T. Ikeda, *J. Mater. Chem.*, 2003, **13**, 2037.
31 B. I. Senyuk, I. I. Smalyukh, and O. D. Lavrentovich, *Opt. Lett.*, 2005, **30**, 349.
32 T. J. White, R. L. Bricker, L. V. Natarajan, N. V. Tabiryan, L. Green, Q. Li, and T. J. Bunning, *Adv. Funct. Mater.*, 2009, **19**, 3484.
33 J. Schmidtke, W. Stille, H. Finkelmann, and S. T. Kim, *Adv. Mater.*, 2002, **14**, 746.
34 P. V. Shibaev, V. I. Kopp, and A. Z. Genack, *J. Phys. Chem. B*, 2003, **107**, 6961.
35 J. D. Lin, M. H. Hsieh, G. J. Wei, T. S. Mo, S. Y. Huang, and C. R. Lee, *Opt. Express*, 2013, **21**, 15765.

Table of contents entry

This work first demonstrates a quantum-dots-embedded cholesteric liquid crystal composite laser added with a chiral-azobenzene with a compatibility of optical stability and reversible tunability.